$[Cr(phen)(ox)_2]^-$: a versatile bis-oxalato building block for the design of heteropolymetallic systems. Crystal structures and magnetic properties of $AsPh_4[Cr(phen)(ox)_2]\cdot H_2O$, $[NaCr(phen)(ox)_2(H_2O)]\cdot 2H_2O$ and $\{[Cr(phen)(ox)_2]_2[Mn_2(bpy)_2(H_2O)_2(ox)]\}\cdot 6H_2O$†

Gabriela Marinescu,[a] Marius Andruh,*[a] Rodrigue Lescouëzec,[b] Mari Carmen Muñoz,[c] Juan Cano,[bd] Francesc Lloret[b] and Miguel Julve*[b]

[a] *Inorganic Chemistry Laboratory, Faculty of Chemistry, University of Bucharest, Str. Drumbrava Rosie nr. 23, 70254 Bucharest, Romania. E-mail: Marius.Andruh@dnt.ro*
[b] *Departament de Química Inorgànica, Facultat de Química de la Universitat de València, Dr. Moliner 50, 46100 Burjassot (València), Spain. E-mail: Miguel.Julve@uv.es*
[c] *Departamento de Física Aplicada, Universidad Politécnica de València, Camino de Vera s/n, 46071 València, Spain*
[d] *Laboratoire de Chimie Inorganique (CNRS UMR 8653), Université de Paris-Sud, 91405 Orsay, France*

Received (in Montpellier, France) 16th March 2000, Accepted 26th April 2000
Published on the Web 21st June 2000

The new complexes of formula $AsPh_4[Cr(phen)(ox)_2]\cdot H_2O$ (**1**), $[NaCr(phen)(ox)_2(H_2O)]\cdot 2H_2O$ (**2**) and $\{[Cr(phen)(ox)_2]_2[Mn_2(bpy)_2(H_2O)_2(ox)]\}\cdot 6H_2O$ (**3**) ($AsPh_4$ = tetraphenylarsonium cation; phen = 1,10-phenanthroline; ox = oxalate dianion; bpy = 2,2′-bipyridine) have been prepared and characterized by single-crystal X-ray diffraction. The structure of **1** consists of discrete $[Cr(phen)(ox)_2]^-$ anions, tetraphenylarsonium cations and uncoordinated water molecules. The chromium environment in **1** is distorted octahedral with Cr–O bond distances between 1.959(3) and 1.947(3) Å and Cr–N bonds of 2.083(4) and 2.072(4) Å. The angles subtended at the chromium atom by the two oxalates are 83.6(2) and 83.3(1)° whereas the N–Cr–N angle is 79.9(2)°. The $[Cr(phen)(ox)_2]^-$ unit of **1** is also present in **2** and **3** but it accomplishes different coordination functions, acting as a bridging (**2**) or terminal (**3**) ligand. **2** has a layered structure made up of oxalato-bridged bimetallic Cr^{III}–Na^{I} helical chains that are interconnected through centrosymmetric Na_2O_2 units. The two oxalates of $[Cr(phen)(ox)_2]^-$ in **2** are bis-chelating within the bimetallic chain but one of them is in addition monodentate towards a sodium atom of a neighbouring chain, yielding a sheetlike structure. The sodium atom in **2** has a distorted octahedral geometry with five Na–O(ox) bonds ranging from 2.453(5) to 2.319(4) Å and the sixth position being occupied by an aqua ligand with Na–O(w) = 2.384(6) Å. The intralayer chromium–sodium and sodium–sodium separations through bridging oxalate in **2** are 5.560(4) and 3.643(8) Å, respectively. The structure of **3** consists of neutral tetranuclear $Cr^{III}_2Mn^{II}_2$ units in which two terminal $[Cr(phen)(ox)_2]^-$ entities act as monodentate ligands towards a central oxalato-bridged manganese(II) dimer. Each manganese atom is six-coordinated as MnN_2O_4 : two nitrogen atoms of a chelating bpy, one aqua ligand and three oxalate oxygens build a distorted octahedron around the manganese atom. The Mn–O(ox) and Mn–N(bpy) bond lengths vary in the ranges 2.219(12)–2.160(13) and 2.33(2)–2.14(2) Å, respectively. The intramolecular chromium–manganese separation [5.507(5) and 5.502(5) Å for Cr(2)···Mn(2) and Cr(1)···Mn(1)] is somewhat shorter that the manganese–manganese one [5.703(2) Å]. The magnetic properties of **1**–**3** have been investigated in the temperature range 1.9–300 K. Very weak antiferromagnetic interactions between the chromium centers are observed in **1** and **2** in agreement with their crystal structures. In the case of **3**, significant intramolecular antiferromagnetic interactions between the adjacent chromium(III) and manganese(II) ions ($j = -1.1$ cm^{-1}, through the chelating/monodentate oxalato) and between the two manganese(II) ions ($J = -2.2$ cm^{-1}, through the bis-chelating oxalato) occur, the Hamiltonian being defined as $\hat{H} = -J\hat{S}_{Mn1}\cdot\hat{S}_{Mn2} - j[\hat{S}_{Cr1}\cdot\hat{S}_{Mn1} + \hat{S}_{Cr2}\cdot\hat{S}_{Mn2}]$.

The use of the tris-chelated species $[M(ox)_3]^{3-}$ (M = trivalent metal ion; ox = oxalate dianion) as ligands towards transition metal ions is well documented in chemistry.[1–4] Its negative charge and the ability of the oxalato to adopt a bis-chelating coordination mode make it a suitable starting material to prepare oxalato-bridged heterometallic compounds with controlled nuclearity and dimensionality.[5–19] A very interesting observation concerning this type of compound is the formation of two- (2D) and three-dimensional (3D) structures depending on the templating counterion. For instance, honeycomb-layered structures of formula $[M^{II}M^{III}(ox)_3]^-$ are obtained when the cation is $[XR_4]^+$ (X = N, P; R = phenyl,

† Three of the authors of the present work (M. Andruh, F. Lloret and M. Julve) were postdoctoral students in Prof. Kahn's laboratory. We are deeply indebted to him because he was not only our scientific father in molecular magnetism but he transmitted his enthusiasm, *savoir faire* and creativity to us. Unfortunately he passed away recently, and the present work is just one of our modest contributions to his living memory.

n-propyl, *n*-butyl, *n*-pentyl) or ferrocenium. However, chiral 3D networks of formula $[M^{II}_2(ox)_3]^{2-}$, $[M^{I}M^{III}(ox)_3]^{2-}$ and $[M^{II}M^{III}(ox)_3]^{-}$ result when the cation is the tris-chelated $[M(bpy)_3]^{m+}$ (bpy = 2,2′-bipyridine; $m = 2$, 3). These supramolecular systems are very interesting not only from a structural point of view, but because of the photochemical, photophysical and magnetic properties that they exhibit, arising from the interaction among their constituents.[1–4,20,21] In the case of $M = Cr^{III}$, the inert character of the tris(oxalato)chromate(III) species makes the preparation of the desired polymetallic compounds easier.[5,6–8,15–17,19,20]

Apart from the homoleptic $[Cr(ox)_3]^{3-}$ species, three heteroleptic and mononuclear oxalato-containing chromium(III) complexes of formula $[Cr(salen)(ox)]^{-}$[22,23] ($salen^{2-}$ = *N*,*N*′-ethylenebis(salicylideneiminate), $[Cr(bpy)(ox)_2]^{-}$[24–27] and $[Cr(bpm)(ox)_2]^{-}$[28,29] (bpm = 2,2′-bipyrimidine) have been used so far to prepare heterometallic compounds. Oxalato-bridged heterobinuclear complexes of the type Cr^{III}–ox–M^{II} (M = Cu, Ni, Co, Fe, Mn) were prepared by reaction of the $[Cr(salen)(ox)]^{-}$ with the divalent cation previously bound to a tri- or terdentate blocking ligand.[23] As far as the second brick is concerned, $[Cr(bpy)(ox)_2]^{-}$, we have recently illustrated its exceptional versatility in designing heterometallic complexes.[24–27] The self-assembly of this mononuclear unit with mono- or dipositive cations led to two series of heteropolynuclear complexes with different stoichiometries: $[M^{I}Cr(bpy)(ox)_2(H_2O)_x]$ (M = Na, Ag)[24,25] and $[M^{II}Cr_2(bpy)_2(ox)_4(H_2O)_y]$ (M = Ba, Mn, Co, Ni, Cu, Zn).[25–27] Within each series, completely different structures are obtained according to the coordination algorithm of the assembling cation. The sodium derivative exhibits a two-dimensional framework with hexa-coordinated sodium atoms,[24] while in the case of silver(I) the structure consists of discrete tetranuclear cycles formed by two chromium and two penta-coordinated silver atoms bridged by the oxalato groups.[25] Within the second series, the barium derivative is a scaffolding-like material with a 3D structure and ten-coordinated barium atoms,[26] the manganese derivative exhibits a new type of heterobimetallic chain with octa-coordinated manganese atoms,[26] whereas the structures of the $\{CoCr_2\}$[26] and $\{CuCr_2\}$[25] complexes consist of discrete, linear $\{Cr^{III}M^{II}Cr^{III}\}$ trinuclear species with hexa-coordinated M^{II} ions. Finally, the hybrid building block $[Cr(bpm)(ox)_2]^{-}$, which can coordinate to the metal ions through both bpm and oxalate, was prepared and structurally characterized.[28] The crystallographic investigation of its sodium[28] and potassium[29] derivatives revealed the occurrence of two different sheetlike polymers of formula $[NaCr(bpm)(ox)_2]\cdot 5H_2O$ and $[K(H_2O)Cr(bpm)(ox)_2]$.

The richness and variety of the structures reported so far induced us to carry out a systematic study of the complexing ability of the bis-oxalato-chromium(III) building block. In this context, we have investigated the coordinating properties of the mononuclear $[Cr(phen)(ox)_2]^{-}$ (phen = 1,10-phenanthroline) species. Our first results concerning the preparation, the structural and magnetic characterization of the complexes of formula $AsPh_4[Cr(phen)(ox)_2]\cdot H_2O$ (**1**) ($AsPh_4$ = tetraphenylarsonium cation), $[NaCr(phen)(ox)_2(H_2O)]\cdot 2H_2O$ (**2**) and $\{[Cr(phen)(ox)_2]_2[Mn_2(bpy)_2(H_2O)_2(ox)]\}\cdot 6H_2O$ (**3**) are presented here. The structures of the heterobimetallic compounds **2** (a sheetlike polymer) and **3** (a tetranuclear complex) illustrate the versatility as a ligand of the $[Cr(phen)(ox)_2]^{-}$ mononuclear complex, which is present in **1**.

Experimental

Materials

1,10-Phenanthroline, 2,2′-bipyridine, chromium(III) chloride hexahydrate, manganese(II) chloride tetrahydrate, sodium oxalate and tetraphenylarsonium chloride monohydrate were purchased from commercial sources and used as received. Elemental analysis (C, H, N) were carried out by the Microanalytical Service of the Universidad Autónoma de Madrid. The Na : Cr (**2**) and Mn : Cr (**3**) ratios were determined by electron microscopy at the Servicio Interdepartamental de Investigación of the University of València.

Preparation of $AsPh_4[Cr(phen)(ox)_2]\cdot H_2O$ (1). An aqueous solution (20 cm^3) containing chromium(III) chloride (1 mmol) and phen (1 mmol) was refluxed under continuous stirring for half an hour. Sodium oxalate (2 mmol), dissolved in a minimum amount of hot water (10 cm^3), was added to the resulting deep green solution and the color turned deep violet under gentle warming and stirring for 20 min. A small amount of a deep violet solid that appeared was removed and discarded. The addition of a concentrated aqueous solution of tetraphenylarsonium chloride (1 mmol, 10 cm^3) caused the crystallization of a first crop of crystals of **1** as violet parallelepipeds on standing at room temperature. Yield *ca.* 35%. Anal. calcd for $C_{40}H_{30}AsCrN_2O_9$ (**1**): C, 59.36; H, 3.71; N, 3.46. Found: C, 59.42; H, 3.45; N, 3.56%.

Preparation of $[NaCr(phen)(ox)_2(H_2O)]\cdot 2H_2O$ (2). Sodium perchlorate (0.1 mmol), dissolved in a minimum amount of water, was added to an aqueous solution of **1** (0.1 mmol, 20 cm^3). The white precipitate of tetraphenylarsonium perchlorate was filtered off and a saturated aqueous solution of NaCl was added to the violet mother liquor. Red prisms of **2** were grown on standing at room temperature. Yield *ca.* 65%. Anal. calcd for $C_{16}H_{14}CrN_2NaO_{11}$ (**2**): C, 39.61; H, 2.89; N, 5.77. Found: C, 39.53; H, 2.80; N, 5.72%.

Preparation of $\{[Cr(phen)(ox)_2]_2[Mn_2(bpy)_2(H_2O)_2(ox)]\}\cdot 6H_2O$ (3). To an aqueous solution of **2** (1 mmol, 20 cm^3) were successively added an aqueous solution of manganese(II) chloride (1 mmol, 10 cm^3), an ethanolic solution of 2,2′-bipyridine (1 mmol, 10 cm^3) and an aqueous solution of sodium oxalate (0.5 mmol, 10 cm^3). The resulting mixture was filtered and left undisturbed. Slow evaporation at room temperature after two weeks afforded a first crop of chunky red purple crystals of **3**. Yield *ca.* 30%. Anal. calcd for $C_{27}H_{24}CrMnN_4O_{14}$ (**3**): C, 44.11; H, 3.26; N, 7.62. Found: C, 44.03; H, 3.10; N, 7.53.%

IR characterisation

The out-of-plane bending vibrations of the phenyl rings of the tetraphenylarsonium cation appear as two sharp and medium intensity peaks at 760 and 750 cm^{-1} in the IR spectrum of **1**. In the 3500 cm^{-1} region, sharp and medium intensity peaks occur in **1** (*ca.* 3495 cm^{-1} with a shoulder at 3550 cm^{-1}), whereas strong and broad absorptions centered at 3440 and 3450 cm^{-1} are observed for **2** and **3**, respectively. These high frequency features are in agreement with the presence of water molecules of crystallization in the former complex and both coordinated and uncoordinated water molecules linked by hydrogen bonds in the two latter ones.[30] Finally, slight but significant differences are observed in the $\nu_{as}(CO)$ stretching region of the IR spectra of **1**–**3**: three strong intensity peaks at 1715, 1700 and 1679 cm^{-1} (**1**), two strong intensity doublets at 1710 and 1675 cm^{-1} (**2**) and three strong peaks at 1710, 1680 and 1639 cm^{-1} (**3**). The different coordination modes of oxalate that occur in **1**–**3** (see structural discussion) account for these spectral differences in the carbonyl vibrations.

Physical techniques

IR spectra (4000–400 cm^{-1}) were recorded on a Bruker IF S55 spectrophotometer with samples prepared as KBr pellets. Variable-temperature (1.9–290 K) magnetic susceptibilty mea-

surements on polycrystalline samples were carried out with a Quantum Design SQUID operating at 0.5 T in the high temperature range (20–290 K) and at 250 G at $T < 20$ K in order to avoid saturation phenomena. Diamagnetic corrections of the constituent atoms were estimated from Pascal's constants[31] as -388×10^{-6} (**1**), -235×10^{-6} (**2**) and -745×10^{-6} (**3**) cm^3 mol^{-1}.

X-Ray data collection and structure refinement

Crystals of dimensions 0.15 × 0.10 × 0.10 (**1**), 0.10 × 0.15 × 0.10 (**2**) and 0.15 × 0.20 × 0.10 mm (**3**) were mounted on an Enraf-Nonius CAD-4 diffractometer and used for data collection. The unit cell parameters were determined from least-squares refinement on the setting angles from 25 centered reflections in the range $12 < \theta < 20°$. A summary of the crystallographic data and structure refinement is given in Table 1. No significant fluctuations were observed in the intensities of three standard reflections monitored periodically thoughout data collection. Intensity data were corrected for Lorentz polarization and absorption corrections.

The structures of **1**–**3** were solved by standard Patterson methods and refined by the full-matrix least-squares method on F^2. All our attempts to solve the structure of **3** in the $P\bar{1}$ space group were unsuccessful. The computations were performed with SHELX 86 and SHELXL 93.[32] All non-hydrogen atoms were refined anisotropically. The hydrogen atoms of the water molecules of **1**–**3** were neither found nor calculated. The hydrogen atoms of the phen (**1**–**3**) and bpy (**3**) ligands were set in calculated positions and refined as riding atoms with a common fixed isotropic thermal parameter.

The final full-matrix least-squares refinement on F^2, minimizing the function $\Sigma w[(|F_o|)^2 - (|F_c|)^2)]^2$ with $w = 1/[\sigma^2(F_o^2) + (mP)^2 + nP]$ and $P = (F_o^2 + 2F_c^2)/3$ [$m = 0.0567$ (**1**), 0.1075 (**2**) and 0.1006 (**3**); $n = 0.3034$ (**1**), 3.4949 (**2**) and 1.9006 (**3**)], converged at the values of R and R_w listed in Table 1. The values of f, f' and f'' were taken from ref. 33. The molecular plots were drawn with the ORTEP program.[34] Selected bond lengths and angles are gathered in Tables 2–4 for **1**–**3**, respectively.

CCDC reference number 440/186.

Results and discussion

Description of the structures

$AsPh_4[Cr(phen)(ox)_2]\cdot H_2O$ (1). The structure of complex **1** consists of tris-chelated $[Cr(phen)(ox)_2]^-$ anions, $AsPh_4^+$ cations and water molecules of crystallization (Fig. 1), which are linked by electrostatic forces and van der Waals interactions.

Each chromium atom is coordinated by two phen nitrogen and four oxalate oxygen atoms, adopting a distorted octahedral geometry. The short bites of bidentate phen and ox ligands [79.90(14), 85.58(13) and 83.38(13)° for N(1)–Cr(1)–N(2), O(1)–Cr(1)–O(2) and O(3)–Cr(1)–O(4), respectively] are the main factors accounting for the distortion of the metal environment from the ideal octahedron. The four Cr–O(ox) bond lengths are very similar [values vary in the range 1.947(3)–1.949(3) Å] and they compare well with the average value reported in the parent mononuclear $[Cr(bpm)(ox)_2]^-$ [1.945(6) Å],[28] $[Cr(bpy)(ox)_2]^-$ [1.953(2) Å][24] and $[Cr(hm)(ox)_2]^-$ [1.974(2) Å][35] (hm = histamine) units. The Cr–N(phen) bond distances [2.082(3) and 2.073(4) Å] are somewhat longer than the Cr–O(ox) ones but they agree with those reported for other phen-containing chromium(III) complexes.[36,37] The phen and ox ligands do not exhibit significant deviations from planarity. The dihedral angle between the two oxalate planes is 89.57(9)° whereas those of phen with the two oxalate planes are 89.67(9) and 88.36(9)°. Bond lengths and angles within the phen ligand are in agreement with those reported for the free phen molecule.[38] The carbon–carbon bond distances in the ox ligand are as expected for single C–C bonds [1.578(7) and 1.559(7) Å for C(13)–C(14) and C(15)–

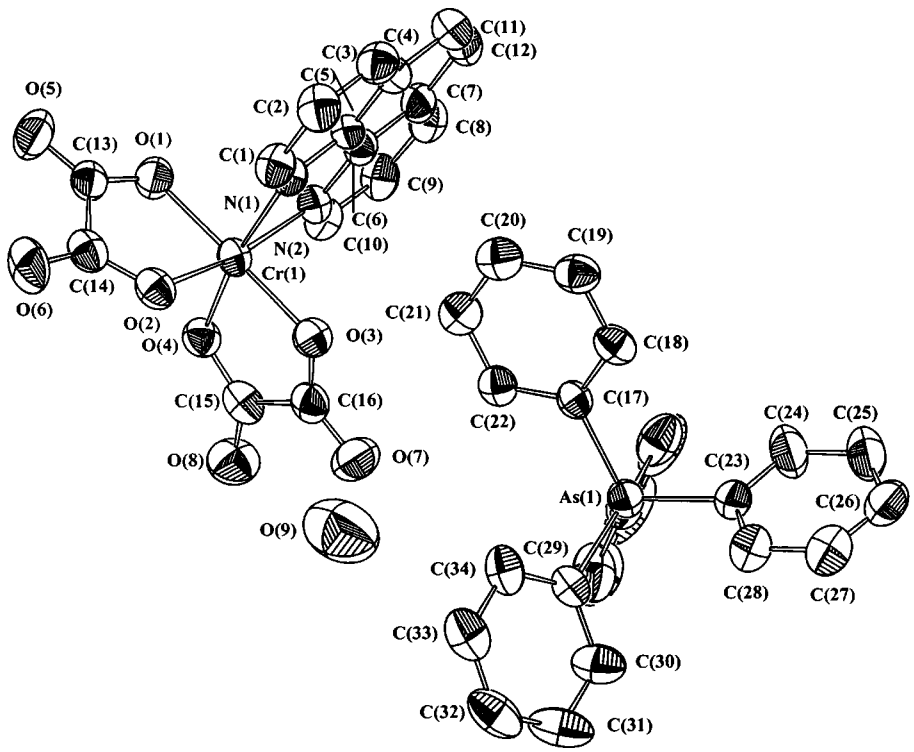

Fig. 1 Perspective view of compound **1** along with the atom numbering. The thermal ellipsoids are drawn at the 30% probability level and the hydrogen atoms have been omitted for clarity.

Table 1 Crystallographic data for $AsPh_4[Cr(phen)(ox)_2]\cdot H_2O$ (**1**), $[NaCr(phen)(ox)_2(H_2O)]\cdot 2H_2O$ (**2**) and $\{[Cr(phen)(ox)_2]_2[Mn_2(bpy)_2(H_2O)_2(ox)]\}\cdot 6H_2O$ (**3**)

	1	**2**	**3**
Formula	$C_{40}H_{30}AsCrN_2O_9$	$C_{16}H_{14}CrN_2NaO_{11}$	$C_{27}H_{24}CrMnN_4O_{14}$
FW	807.56	970.56	744.45
Crystal system	Triclinic	Monoclinic	Triclinic
Space group	$P\bar{1}$(no. 2)	$P2_1/n$(no. 14)	$P1$(no. 1)
a/Å	9.503(2)	9.092(2)	9.014(2)
b/Å	14.264(4)	13.828(2)	10.0404(11)
c/Å	14.642(3)	15.882(2)	18.445(2)
α/°	103.34(2)	90.0	79.343(10)
β/°	99.51(2)	92.977(14)	77.989(13)
γ/°	106.43(2)	90.0	86.773(13)
U/Å^3	1794.9(7)	1994.0(5)	1604.4(4)
Z	2	4	2
T/K	293(2)	293(2)	293(2)
μ(Mo-Kα)/cm^{-1}	12.94	6.59	8.07
No. measd. ind. refl.	4649	3504	4498
No. obsd. refl. [$I \geqslant 2\sigma(I)$]	4627	3437	4455
R^a	0.0419	0.0638	0.0506
$R_w{}^b$	0.0941	0.1728	0.1301

[a] $R = \Sigma(\|F_o| - |F_c\|)/\Sigma|F_o|$. [b] $R_w = [\Sigma w(|F_o|^2 - |F_c|^2)^2]/\Sigma w|F_c|^2]^{1/2}$.

Table 2 Selected bond lengths (Å) and angles (deg)[a] for compound **1**

Cr(1)–N(1)	2.073(4)	Cr(1)–N(2)	2.082(3)
Cr(1)–O(1)	1.956(3)	Cr(1)–O(2)	1.956(3)
Cr(1)–O(3)	1.959(3)	Cr(1)–O(4)	1.947(3)
N(1)–Cr(1)–O(1)	91.13(13)	N(1)–Cr(1)–O(2)	93.22(13)
N(1)–Cr(1)–O(3)	89.34(13)	N(1)–Cr(1)–N(2)	79.90(14)
N(1)–Cr(1)–O(4)	169.86(13)	N(2)–Cr(1)–O(1)	89.89(13)
N(2)–Cr(1)–O(2)	170.44(14)	N(2)–Cr(1)–O(3)	91.73(13)
N(2)–Cr(1)–O(4)	93.22(13)	O(1)–Cr(1)–O(2)	83.58(13)
O(1)–Cr(1)–O(3)	178.38(13)	O(1)–Cr(1)–O(4)	96.34(13)
O(2)–Cr(1)–O(3)	94.84(13)	O(2)–Cr(1)–O(4)	94.42(13)
O(3)–Cr(1)–O(4)	83.38(13)		

[a] Estimated standard deviations in the last significant digits are given in parentheses.

Table 3 Selected bond lengths (Å) and angles (deg)[a,b] for compound **2**

Chromium environment			
Cr(1)–N(1)	2.077(4)	Cr(1)–N(2)	2.068(4)
Cr(1)–O(1)	1.954(3)	Cr(1)–O(2)	1.956(3)
Cr(1)–O(3)	1.955(3)	Cr(1)–O(4)	1.949(3)
N(1)–Cr(1)–O(1)	92.90(14)	N(1)–Cr(1)–O(3)	91.7(2)
N(1)–Cr(1)–O(4)	91.9(2)	N(1)–Cr(1)–N(2)	79.88(14)
N(1)–Cr(1)–O(2)	172.26(14)	N(2)–Cr(1)–O(1)	91.8(2)
N(2)–Cr(1)–O(3)	170.9(2)	N(2)–Cr(1)–O(4)	93.60(14)
N(2)–Cr(1)–O(2)	93.8(2)	O(1)–Cr(1)–O(3)	92.21(14)
O(1)–Cr(1)–O(4)	173.4(2)	O(1)–Cr(1)–O(2)	82.81(13)
O(3)–Cr(1)–O(4)	83.06(14)	O(3)–Cr(1)–O(2)	94.9(2)
O(4)–Cr(1)–O(2)	92.9(2)		
Sodium environment			
Na(1)–O(5*a*)	2.319(4)	Na(1)–O(5*b*)	2.445(4)
Na(1)–O(6*a*)	2.418(5)	Na(1)–O(7)	2.403(4)
Na(1)–O(8)	2.453(5)	Na(1)–O(9)	2.384(6)
O(5*a*)–Na(1)–O(5*b*)	80.22(14)	O(5*a*)–Na(1)–O(6*a*)	68.94(13)
O(5*a*)–Na(1)–O(8)	84.4(2)	O(5*a*)–Na(1)–O(9)	117.2(3)
O(5*a*)–Na(1)–O(7)	139.6(2)	O(6*a*)–Na(1)–O(7)	81.9(2)
O(6*a*)–Na(1)–O(8)	91.2(2)	O(6*a*)–Na(1)–O(9)	96.0(3)
O(6*a*)–Na(1)–O(5*b*)	149.1(2)	O(7)–Na(1)–O(8)	68.36(14)
O(7)–Na(1)–O(9)	92.4(2)	O(7)–Na(1)–O(5*b*)	126.0(2)
O(8)–Na(1)–O(5*b*)	88.2(2)	O(8)–Na(1)–O(9)	158.3(3)
O(9)–Na(1)–O(5*b*)	95.9(2)	Na(1)–O(5*b*)–Na(1*b*)	99.78(14)

[a] Estimated standard deviations in the last significant digits are given in parentheses. [b] Symmetry code: (*a*) $x + 1/2, y - 1/2, -z + 1/2$; (*b*) $x - 1/2, -y + 1/2, z + 1/2$.

Table 4 Selected bond lengths (Å) and angles (deg)[a] for compound **3**

Chromium environment			
Cr(1)–N(7)	2.05(2)	Cr(2)–N(5)	2.06(2)
Cr(1)–N(8)	2.07(2)	Cr(2)–N(6)	2.10(2)
Cr(1)–O(16)	1.969(12)	Cr(2)–O(8)	1.957(13)
Cr(1)–O(17)	2.029(13)	Cr(2)–O(9)	1.923(14)
Cr(1)–O(19)	1.92(2)	Cr(2)–O(11)	1.939(14)
Cr(1)–O(21)	1.97(2)	Cr(2)–O(13)	1.97(2)
N(7)–Cr(1)–O(17)	85.9(6)	N(5)–Cr(2)–O(11)	90.7(6)
N(7)–Cr(1)–N(8)	80.7(7)	N(5)–Cr(2)–N(6)	80.0(7)
N(7)–Cr(1)–O(19)	173.2(7)	N(5)–Cr(2)–O(8)	175.5(7)
N(7)–Cr(1)–O(16)	92.8(6)	N(5)–Cr(2)–O(13)	93.2(6)
N(7)–Cr(1)–O(21)	95.1(6)	N(5)–Cr(2)–O(9)	94.7(6)
N(8)–Cr(1)–O(17)	92.4(6)	N(6)–Cr(2)–O(11)	89.9(7)
N(8)–Cr(1)–O(16)	171.4(6)	N(6)–Cr(2)–O(13)	171.3(13)
N(8)–Cr(1)–O(21)	92.4(6)	N(6)–Cr(2)–O(9)	94.5(6)
N(8)–Cr(1)–O(19)	92.9(6)	N(6)–Cr(2)–O(8)	96.3(6)
O(16)–Cr(1)–O(19)	93.8(6)	O(8)–Cr(2)–O(13)	90.7(7)
O(16)–Cr(1)–O(17)	81.9(6)	O(8)–Cr(2)–O(11)	91.7(6)
O(16)–Cr(1)–O(21)	93.8(6)	O(8)–Cr(2)–O(9)	83.1(6)
O(19)–Cr(1)–O(17)	93.0(6)	O(13)–Cr(2)–O(11)	84.7(7)
O(19)–Cr(1)–O(21)	82.9(6)	O(13)–Cr(2)–O(9)	91.5(6)
O(17)–Cr(1)–O(21)	173.8(6)	O(9)–Cr(2)–O(11)	173.6(6)
Manganese environment			
Mn(1)–N(1)	2.14(2)	Mn(2)–N(3)	2.238(14)
Mn(1)–N(2)	2.20(2)	Mn(2)–N(4)	2.33(2)
Mn(1)–O(1)	2.169(14)	Mn(2)–O(3)	2.19(2)
Mn(1)–O(2)	2.219(12)	Mn(2)–O(4)	2.210(14)
Mn(1)–O(5)	2.21(2)	Mn(2)–O(6)	2.17(2)
Mn(1)–O(15)	2.160(13)	Mn(2)–O(7)	2.211(13)
N(1)–Mn(1)–N(2)	73.6(6)	N(3)–Mn(1)–N(4)	73.8(6)
N(1)–Mn(1)–O(5)	168.4(7)	N(3)–Mn(2)–O(4)	165.0(6)
N(1)–Mn(1)–O(1)	95.1(7)	N(3)–Mn(2)–O(6)	96.3(6)
N(1)–Mn(1)–O(2)	94.8(6)	N(3)–Mn(2)–O(3)	94.5(5)
N(1)–Mn(1)–O(15)	97.0(6)	N(3)–Mn(2)–O(7)	100.1(5)
N(2)–Mn(1)–O(5)	95.2(6)	N(4)–Mn(2)–O(4)	93.8(6)
N(2)–Mn(1)–O(1)	165.8(6)	N(4)–Mn(2)–O(6)	169.6(6)
N(2)–Mn(1)–O(2)	97.9(5)	N(4)–Mn(2)–O(3)	94.2(5)
N(2)–Mn(1)–O(15)	98.0(5)	N(4)–Mn(2)–O(7)	95.5(5)
O(5)–Mn(1)–O(1)	96.5(7)	O(4)–Mn(2)–O(6)	96.4(6)
O(5)–Mn(1)–O(2)	89.9(6)	O(4)–Mn(2)–O(3)	77.6(5)
O(5)–Mn(1)–O(15)	81.1(6)	O(4)–Mn(2)–O(7)	89.4(5)
O(1)–Mn(1)–O(2)	74.0(5)	O(6)–Mn(2)–O(3)	89.9(5)
O(1)–Mn(1)–O(15)	91.9(5)	O(6)–Mn(2)–O(7)	82.7(5)
O(2)–Mn(1)–O(15)	162.4(5)	O(3)–Mn(2)–O(7)	164.2(5)

[a] Estimated standard deviations in the last significant digits are given in parentheses.

C(16), respectively]. The average values for the peripheral and inner C–O bonds are 1.213(5) and 1.295(3) Å, respectively, the shorter values being due to the greater double bond character of the free C–O bonds. The uncoordinated water molecule [O(9)] interacts only very weakly with the oxalate oxygens O(1) and O(4): the O(9)···O(1) and O(9)···O(4) distances are 3.120(2) and 3.405(2) Å, values that are somewhat greater than the sum of the van der Waals radii. The bulky tetraphenylarsonium cation exhibits the expected tetrahedral shape and its bond distances and angles are in agreement with those observed in previous $AsPh_4^+$-containing compounds.[24,28,39] Interestingly, alternating sextuple and double phenyl embraces[40,41] between the $AsPh_4^+$ cations occur along the *z* axis (see Fig. 2), the arsonium–arsonium distances involved being 6.209(2) [As(1)···As(1*a*); (*a*) = $-x$, $1-y$, $1-z$] and 8.736(4) Å [As(1)···As(1*b*); (*b*) = $-x$, $1-y$, $2-z$], respectively. In this latter case, where the offset face-to-face interaction occurs between two phenyl rings of two adjacent cations, the interplanar distance is 3.85(9) Å. In addition, the two phen ligands of two adjacent $[Cr(phen)(ox)_2]^-$ units exhibit a significant graphite-like interaction (see Scheme 1), the separation between the two somewhat slipped phen planes being 3.53(9) Å. The separation between the chromium atoms within this couple is 8.721(6) Å [Cr(1)···Cr(1*c*); (*c*) = $-x$, $-y$, $-z$]. The shortest intermolecular chromium–chromium and chromium–arsonium distances are 7.052(2) [Cr(1)···Cr(1*d*); (*d*) = $1-x$, $-y$, $-z$] and 7.587(2) Å [Cr(1)···As(1*a*)].

$[NaCr(phen)(ox)_2(H_2O)]\cdot 2H_2O$ (2). Complex **2** has an extended two-dimensional structure made up by bimetallic oxalato-bridged Cr^{III}–Na^{I} helical chains (Fig. 3), which are linked through centrosymmetric Na_2O_2 units (see Fig. 4). The resulting sheetlike polymer grows in the *yz* plane. Because of the inversion center, the chromium complexes of neighbouring chains have opposite chirality. The sheets are eclipsed to each other and the intersheet separation is 9.092(2) Å. Hydrogen bonds involving one of the oxalate oxygens [O(8)] and both the coordinated [O(9)] and uncoordinated [O(10) and O(11)] water molecules [values of 2.785(11) and 2.82(3) Å for the O(8)···O(11) and O(9)···O(10) distances, respectively] play an important stabilizing role in the crystal packing energy. Within a sheet, four octanuclear Cr_4Na_4 rings and four tetranuclear Cr_2Na_2 rhombuses alternate regularly around each

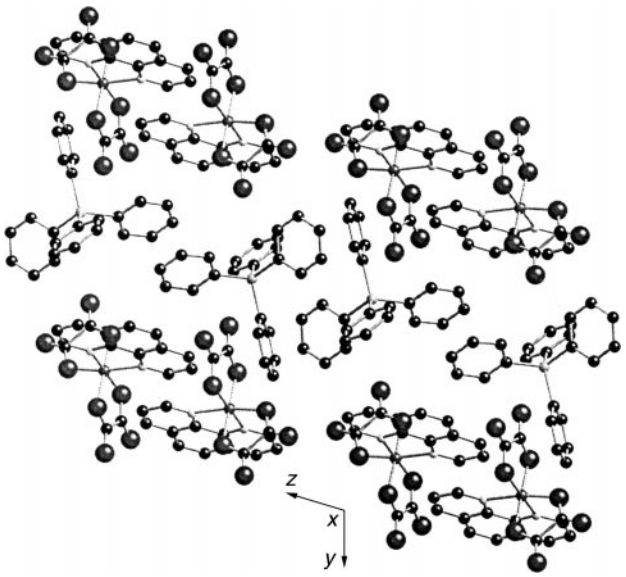

Fig. 2 A projection of the crystal packing of **1** down the *x* axis. The water molecules have been omitted for clarity.

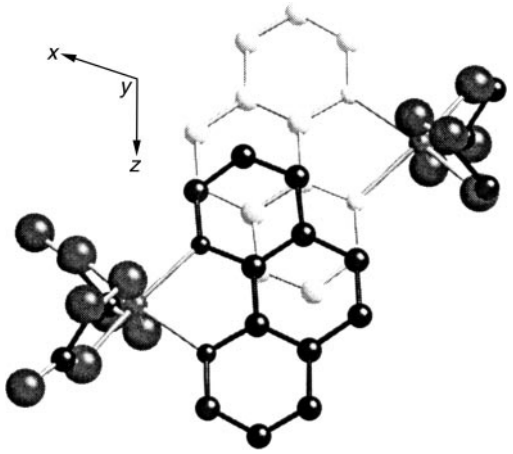

Scheme 1

Cr_4Na_4 unit (see Fig. 5), with a four-fold axis passing through the middle point between two opposite chromium atoms. This topology was also observed in the complex of formula $[NaCr(bpy)(ox)_2(H_2O)]\cdot 2H_2O$[24] where the phen ligand of **2** is replaced by bpy. The main difference between these two compounds is the presence in the bpy derivative of two crystallographically independent tris-chelated chromium atoms, which alternate regularly in each Cr^{III}–Na^{I} bimetallic chain. The octanuclear holes are filled by two phen ligands, which do not exhibit any π–π interaction, the separation between the two phen planes being *ca.* 5 Å.

Each chromium atom in **2** exhibits a distorted octahedral environment, the bond lengths and angles around the metal atom being very close to those observed in **1** (see Table 3). The sodium atom is also six-coordinated with a water oxygen [2.384(6) Å for Cr(1)–O(9)] and five oxalate oxygen atoms

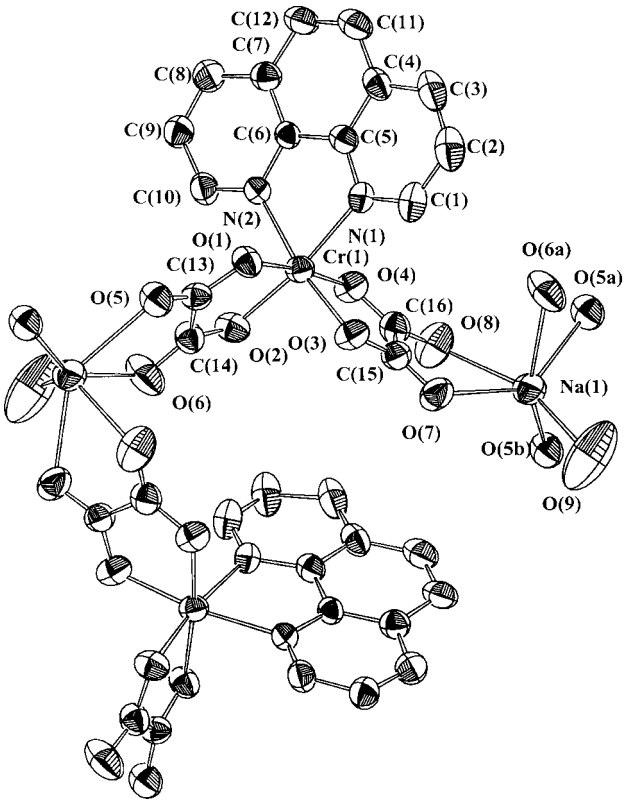

Fig. 3 Perspective view of two symmetry-related units of complex **2** with the atom numbering. The thermal ellipsoids are drawn at the 30% probability level and the hydrogen atoms as well as the hydration water molecules have been omitted for clarity.

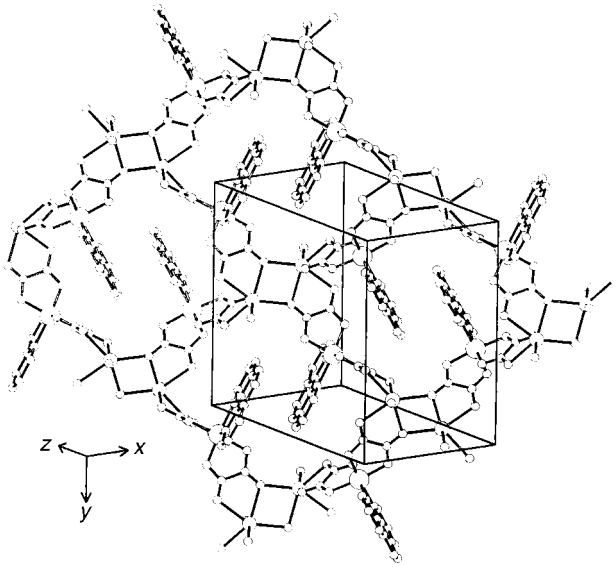

Fig. 4 Perspective drawing of a fragment of a sheet of compound **2** showing the $Cr^{III}_4Na^{I}_4$ cavities partially filled with two phen ligands.

[Cr–O(ox) bond lengths varying in the range 2.453(5)–2.319(4) Å] building a very distorted octahedron. These values compare well with those observed for the sodium atom in the layered $[NaCr(bpy)(ox)_2(H_2O)]\cdot 2H_2O$[24] and $[N(CH_3)_3Ph][NaCr(ox)_3]_2Cl\cdot 5H_2O$[11] compounds as well as

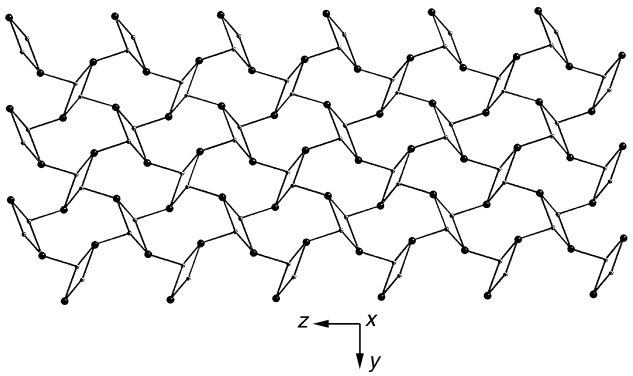

Fig. 5 A topological drawing of one layer of compound **2** showing the alternating arrangement of the Cr_4Na_4 octogons and Na_2O_2 rhombuses. Only the chromium (black circles) and sodium (open circles) atoms are shown for simplicity.

in the three-dimensional $[Fe(bpy)_3][NaFe(ox)_3]$[9] and $[M^{III}(bpy)_3][NaCr(ox)_3]X$ with M = Cr ($X = ClO_4^-$) or Co ($X = PF_6^-$).[15]

As in **1**, neither phen nor ox ligands exhibit significant deviations from planarity. The dihedral angle between the two ox ligands is 85.3(3)° and those of phen with the two oxalate groups are 88.9(2) and 89.7(2)°. The oxalate groups in **2** are bisbidentate but one of them also acts as a monodentate ligand through one of its oxygen atoms [O(5)]. Consequently, each sodium atom is surrounded by two five- [from two oxalate ligands] and one four-membered chelate rings [Na(1)–O(5*a*)–Na(1*c*)–O(5*b*); (*c*) = $-x$, $-y$, $-z+1$]. The Na_2O_2 units are planar and the Na(1)···Na(1*c*) separation is 3.643(8) Å. The chromium–sodium separation through bridging oxalate is 5.560(4) Å. The shortest intra- and intersheet chromium–chromium separations are 7.658(9) [Cr(1)···Cr(1*d*); (*d*) = $1/2-x$, $1/2+y$, $1/2-z$] and 8.141(9) Å [Cr(1)···Cr(1*e*); (*e*) = $1-x$, $1/2-y$, $1/2+z$].

$\{[Cr(phen)(ox)_2]_2[Mn_2(bpy)_2(H_2O)_2(ox)]\}\cdot 6H_2O$ (3). The structure of complex **3** consists of neutral $[Cr(phen)(ox)_2]_2[Mn_2(bpy)_2(H_2O)_2(ox)]$ tetranuclear units (Fig. 6) and water molecules of crystallization linked by van der Waals interactions and an extensive network of hydrogen bonds. Two $[Cr(phen)(ox)_2]^-$ entities act as monodentate ligands through an oxalate oxygen atom, O(15) [at Cr(1)] and O(7) [at Cr(2)], towards a central μ-oxalatobis[(aqua)(2,2′-bipyridyl)manganese(II)] unit. The peripheral chromium complexes are *trans* with respect to the central dinuclear manganese(II) moiety. The most striking feature of the present structure is the occurrence of three different coordination modes of oxalate in the same complex: the usual bisbidentate (between the two manganese atoms) and bidentate (peripheral chromium atoms) coordination modes together with the unprecedented simultaneously bidentate (towards chromium) and monodenate (towards manganese) bridging mode.

The two crystallographically independent chromium atoms exhibit a distorted octahedral environment with bond lengths and angles very similar to each other, the main differences being the lengthening of one of the Cr–O(ox) bonds whose value [2.029(13) Å for Cr(1)–O(17)] is significantly above the remaining ones at either Cr(1) [1.97(2)–1.92(2) Å] or Cr(2) [1.97(2)–1.923(14) Å]. Apart from this detail, the bond lengths and angles around the chromium atoms in **3** agree well with those observed in the structures of **1** and **2**. The phen and ox ligands around Cr(1) and Cr(2) are planar as expected. The dihedral angle between the oxalate planes is 79.8(6)° [at Cr(1)]

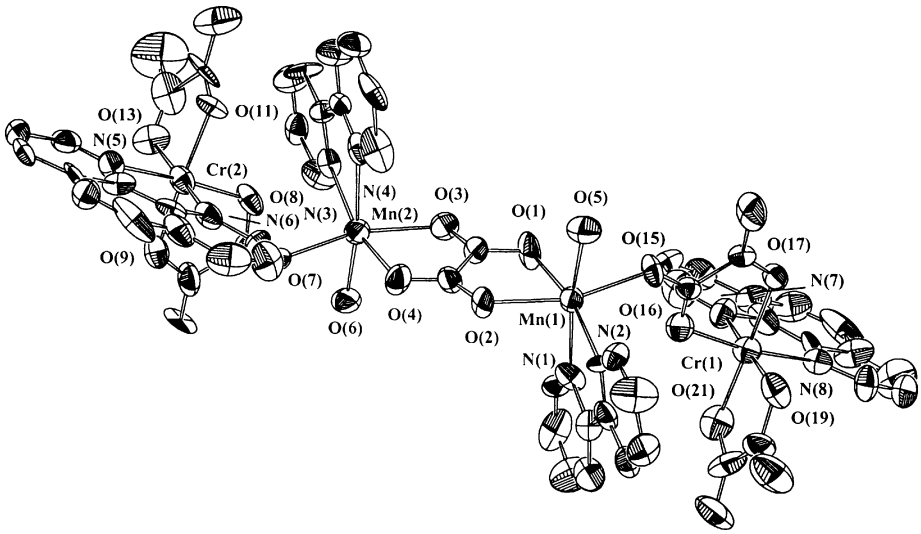

Fig. 6 Perspective drawing of the neutral Cr^{III}–Mn^{II}–Mn^{II}–Cr^{III} tetranuclear unit of complex **3** with the atom numbering. The thermal ellipsoids are drawn at the 30% probability level and the hydrogen atoms have been omitted for clarity.

and 79.4(7)° [at Cr(2)], whereas those between phen and oxalate are 80.9(4) and 79.8(6)° [at Cr(1)] and 87.0(6) and 82.9(4)° [at Cr(2)]. The average carbon–carbon bond lengths of the oxalate ligands bound to the chromium atoms is 1.55(5) Å, a value that is as expected for a single C–C bond. The values of the free C–O oxalate bonds are shorter [values varying in the ranges 1.23(3)–1.20(2) for Cr(1) and 1.25(3)–1.18(3) Å for Cr(2)] than those coordinated to the chromium [the average values for Cr–O are 1.27 Å at Cr(1) and 1.32 Å at Cr(2)].

The two crystallographically independent manganese atoms are also six coordinated: two nitrogen atoms from a bidentate bpy, a water oxygen and three oxalate oxygen atoms (two of a bis-chelating oxalate and one of the terminal $[Cr(phen)(ox)_2]^-$ unit) form a distorted octahedron around each manganese atom. The short bites of the bpy [73.6(6)° at Mn(1) and 73.8(6)° at Mn(2)] and ox [74.0(5) at Mn(1)° and 77.6(5)° at Mn(2)] ligands are the main factors for the distortion of the MnN_2O_4 chromophores. The values of the Mn–N(bpy) bond lengths are somewhat shorter for Mn(1) [2.14(2) and 2.20(2) Å] than for Mn(2) [2.238(14) and 2.33(2) Å] but they compare well with the values reported for other bpy- and carboxylato-containing manganese(II) complexes.[42] The bis-chelating oxalato ligand is asymmetrically coordinated to the manganese atoms [2.169(14) and 2.219(12) Å at Mn(1) and 1.19(2) and 2.210(14) Å at Mn(2)]. This structural fact is in agreement with the results of the X-ray data of other oxalato-bridged manganese(II) complexes such as $[Mn(bpy)(ox)]$,[42b] $[Mn(ox)(H_2O)_2]$[43] and $[Mn_3(ox)_4(H_2O)_2]^{2-}$.[44] The value of the remaining Mn–O(ox) bond involving the oxalato oxygen of the terminal chromium complex [2.160(13) and 2.211(13) Å for Mn(1)–O(15) and Mn(2)–O(7), respectively] compares well with previous structures. The Mn–O(w) bond distances [2.21(2) and 2.17(2) Å for Mn(1)–O(5) and Mn(2)–O(6)] lie within the range of the Mn–O(ox) distances. The bond lengths and angles within the two bidentate bpy ligands are as observed in the free molecule.[45] The two bpy ligands are approximately planar, the dihedral angles between the two pyridyl rings being equal to 3(1)° [(N(1)/N(2) and (N(3)/N(4)]. There are no unusual bond lengths or angles in the planar bis-chelating oxalate. It forms dihedral angles of 86.8(4) and 85.9(3)° with the mean planes of the two bpy ligands and of 87.7(4) and 85.1(4)° with those of the two chelating/monodentate oxalates [O(3)/O(7) and O(3)/O(15)]. Finally, the dihedral angle between mean planes of the N(1)/N(2) bpy and O(15)-containing oxalate is 85.1(6)°, a value very close to that of N(3)/N(4) bpy and the O(7)-containing oxalate [85.8(5)°].

The intramolecular metal–metal separations are 5.703(2) [Mn(1)···Mn(2)], 5.502(5) [Mn(1)···Cr(1)], 5.507(5) [Mn(2)···Cr(2)], 9.957(5) [Mn(1)···Cr(2)], 9.952(5) [Mn(2)···Cr(1)] and 15.042(3) Å [Cr(1)···Cr(2)], whereas the shortest intermolecular separations are 5.927(2) [Mn(1)···Mn(2*a*); (*a*) = 1 + *x*, *y*, *z*] and 9.014(2) Å [Mn(1)···Mn(1*a*), Mn(2)···Mn(2*a*), Cr(1)···Cr(1*a*) and Cr(2)···Cr(2*a*)]. Significant π–π interactions between bpy ligands [interplanar distance of 3.7(2) Å] of neighbouring tetranuclear units are observed whereas much weaker π–π interactions occur between the phen groups [the shortest interplanar phen–phen separation is 4.7(2) Å] (see Fig. 7). An extensive network of hydrogen bonds involving the six uncoordinated water molecules and some of the oxalato oxygens are also present [2.61(2), 2.65(4), 2.74(4), 2.78(2), 2.82(3) and 2.93(2) Å for O(20)···O(27), O(23)···O(28), O(12)···O(24), O(4)···O(25), O(22)···O(23) and O(18)···O(26), respectively].

Magnetic properties of 1–3

The temperature dependence of $\chi_M T$ for **1** and **2** [χ_M being the magnetic susceptibility per mole of chromium(III)] in the temperature range 1.9–100 K is shown in Fig. 8. Both curves are quite similar. $\chi_M T$ at 290 K is equal to 1.85 $cm^3\ mol^{-1}$ K (**1** and **2**), a value which is as expected for a magnetically isolated spin quartet (the calculated value of $\chi_M T$ for $S = 3/2$ with $g = 2.0$ is 1.88 $cm^3\ mol^{-1}$ K). This value remains practically unchanged when cooling and it decreases smoothly in the lower temperature region, the curve of **1** being slightly below that of **2** (the $\chi_M T$ values for **1** and **2** at 2.0 K are 1.43 and 1.74 $cm^3\ mol^{-1}$ K, respectively). No susceptibility maximum was observed for **1** or **2** in the temperature range explored. The decrease of $\chi_M T$ in the lower temperature range for both complexes can be due to the zero field splitting (*D*) of the chromium(III) ion, to weak antiferromagnetic interactions between the local spin quartets or both of these. Keeping in mind the mononuclear nature of **1**, we have analyzed its mag-

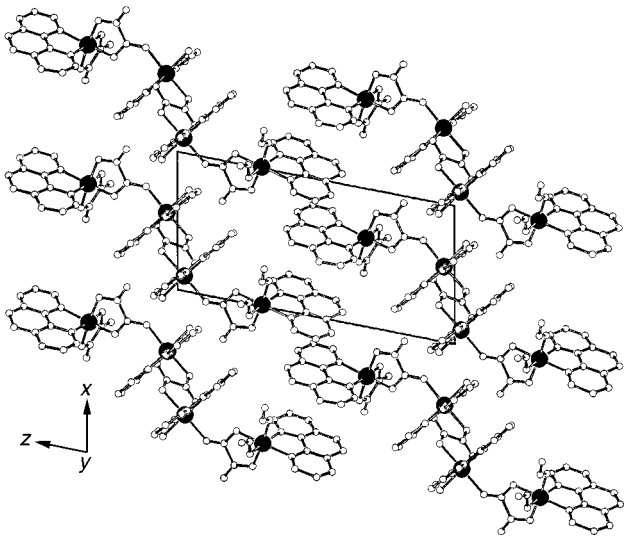

Fig. 7 Projection of the packing of complex **3** along the *y* axis. Black circles represent the metal ions.

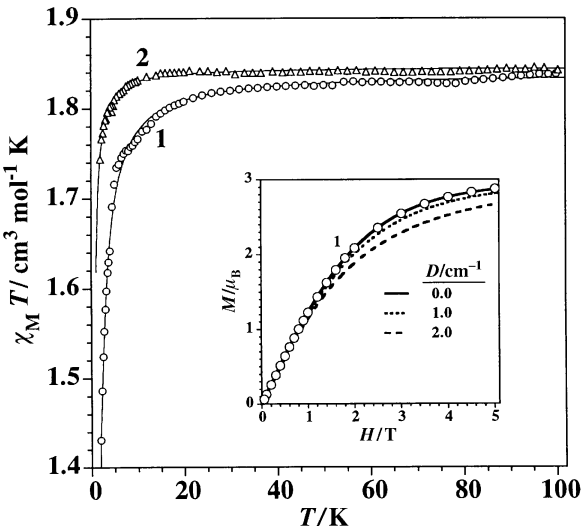

Fig. 8 $\chi_M T$ *vs.* *T* plot for **1** (○) and **2** (△). The solid lines correspond to the best fit through the corresponding expressions (see text). The inset shows the magnetization *vs.* the applied magnetic field at 2.0 K for **1**: (○) experimental data; (——), (·····) and (– – –) calculated curves for a magnetically isolated spin of $S = 3/2$ with *D* values of 0.0, 1.0 and 2.0 cm^{-1}, respectively.

netic data through eqn. (1),[46] which is derived from the

$$\chi_M = \frac{N\beta^2 g^2}{3kT}(\chi_{\|} + 2\chi_{\perp}) \quad (1)$$

$$\chi_{\|} = \frac{1 + 9\exp(-2D/kT)}{4(1 + \exp(-2D/kT)} \quad (2)$$

$$\chi_{\perp} = \frac{4 + (3kT/D)[1 - \exp(-2D/kT)]}{4[1 + 2\exp(-2D/kT)]} \quad (3)$$

$$\hat{H} = D[\hat{S}_Z^2 - \tfrac{1}{3}S(S+1)] \quad (4)$$

Hamiltonian given by eqn. (4), where we have considered an axial zero field splitting and $S = 3/2$. Least-squares fit of the susceptibility data of **1** through eqn. (1) leads to $D = 2.7$ cm^{-1} and $g = 1.98$, the agreement with the calculated and theoretical data being quite good. Assuming that the decrease of the susceptibility data of **1** is only due to intermolecular interactions (θ), D is made equal to zero in eqns. (1)–(3) and T is replaced by $T - \theta$ in eqn. (1). Least-squares fit through the modified expression of eqn. (1), where the variable parameters are θ and g, leads to $\theta = -0.5$ K and $g = 1.98$, the quality of the fit being as good as the preceding one. To evaluate the magnitude of D, we have measured the magnetization curve of **1** as a function of the field at 2.0 K which is shown in the inset of Fig. 8. An inspection of this curve shows that the magnetization data are well reproduced by a curve with $D = 0$ cm^{-1} and $g = 1.97$ (the curves for D values of 1 and 2 cm^{-1} are clearly below the experimental data). The slightly smaller value of g (<1.98–1.99, expected for Cr^{III}) may be due to the occurrence of weak intermolecular magnetic interactions. In summary, the fit with D *ca.* zero and $\theta = -0.5$ K is the best for the magnetization curve of **1**. Given that $\theta = zJS(S+1)/3k$ and that $S = 3/2$ in the present case, $zJ = -0.9$ cm^{-1}. As the packing of **1** shows that pairs of tris-chelated chromium(III) units are present (through a weak π–π phen–phen overlap), z is equal to 1 and consequently, $J = -0.9$ cm^{-1}. In accord with this reasoning, a weak magnetic interaction through π stacking was reported previously.[47] This value of J is the upper limit for the magnetic coupling in **1** given that a very small but non-zero value of the zero-field splitting may be involved. In the case of the magnetic properties of **2**, we analyzed them through eqn. (1) with D and g as the variable parameters and further, setting D equal to zero and replacing T by $T - \theta$ in eqn. (1). Least-squares fits led to $g = 1.98$ in both cases, the values of D and θ being 0.1 cm^{-1} and −0.1 K, respectively. Taking into account that within a sheet in **2**, the chromium atoms describe a square lattice ($z = 4$), a value of $J = -0.02$ cm^{-1} (this value being the upper value of the magnetic interaction in **2** as mentioned above for **1**) is easily obtained from that of θ. Finally, the treatment of the susceptibility data of **2** through the Lines model for an isotropic square lattice with local spins $S = 3/2$,[48] leads to $J = -0.014$ cm^{-1} and $g = 1.98$. The quality of the three fits is very similar and the computed g value is the same in the three models. However, the fact that the D value is practically zero in **1** and the occurrence of the same environment for the chromium atom in **1** and **2**, induce us to attribute the slight decrease of $\chi_M T$ in **2** to weak intrasheet antiferromagnetic interactions between chromium(III) ions separated by more than 7.6 Å.

The temperature dependence of $\chi_M T$ for **3** (χ_M is the magnetic susceptibility per $Cr_2^{III}Mn_2^{II}$ unit) in the temperature range 2.0–300 K is shown in Fig. 9. At room temperature, $\chi_M T$ is equal to 11.8 cm^3 mol^{-1} K, a value which is somewhat smaller than the expected one for two chromium(III) and two manganese(II) ions without any magnetic interaction [$\chi_M T$ = 12.4 cm^3 mol^{-1} K with $g_{Cr} = g_{Mn} = 2.00$]. This value

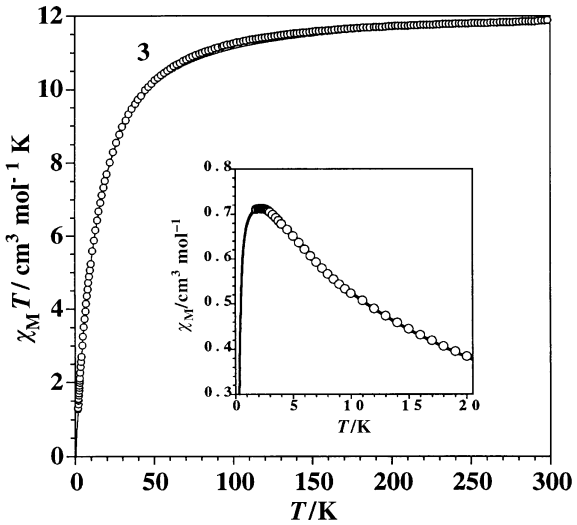

Fig. 9 $\chi_M T$ *vs.* T plot for **3**: (○) experimental data; (——) best fit through eqn. (5). The inset shows the susceptibility curve in the low temperature region.

decreases sharply when cooling and attains a value of 1.50 cm^3 mol^{-1} K at 2.0 K. The susceptibility curve exhibits an incipient maximum at 2.5 K (see inset of Fig. 9). These features are indicative of the occurrence of an overall antiferromagnetic behaviour of complex **3**. Keeping in mind its crystal structure (tetranuclear unit with two types of bridging oxalate), we analyzed the susceptibility data through the simplified isotropic Hamiltonian of eqn. (5)

$$\hat{H} = -J\hat{S}_{Mn1}\cdot\hat{S}_{Mn2} - j[\hat{S}_{Cr1}\cdot\hat{S}_{Mn1} + \hat{S}_{Cr2}\cdot\hat{S}_{Mn2}] \quad (5)$$

where J is the magnetic interaction through bis-chelating oxalato (inner manganese pair) and j represents the magnetic coupling through chelating/monodentate oxalato (each peripheral chromium atom with its adjacent manganese atom). The interactions between peripheral chromium atoms and those of each chromium atom with its non-adjacent manganese atom are neglected and the two peripheral chromium atoms are assumed to be identical. The best agreement between the experimental and calculated data is obtained for $J = -2.2$ cm^{-1}, $j = -1.1$ cm^{-1}, $g_{Mn} = 1.99$ and $g_{Cr} = 1.98$ with $R = 1.0 \times 10^{-5}$ where R is the agreement factor defined as $\Sigma_i[(\chi_M T)_{obs}(i) - (\chi_M T)_{calc}(i)]^2/\Sigma[(\chi_M T)_{obs}(i)]^2\}$. The theoretical curve (solid line in Fig. 9) matches very well the experimental data.

The value of the antiferromagnetic coupling between the two manganese(II) ions through the bischelating oxalato ligand in **3** ($J = -2.2$ cm^{-1}) is in agreement with those reported for other oxalato-bridged manganese(II) compounds (values of the magnetic coupling range from −1.8 to −2.5 cm^{-1}).[42c,49,50] The exchange pathway for this significant antiferromagnetic interaction between paramagnetic centres through bis-chelating oxalato is well known[51] and several theoretical papers have been devoted to its analysis.[52–54] In fact, the good overlap between the two $d_{x^2-y^2}$ type metal-centred magnetic orbitals [the x and y axes being roughly defined by the Mn(1)–O(1) and Mn(1)–O(2) bonds] accounts for the antiferromagnetic interaction observed. As far as the exchange coupling between the Cr^{III} and Mn^{II} through the chelating/monodentate bridging oxalate ($j = -1.1$ cm^{-1}) is concerned, no previous magneto-structural data are available to our knowledge. Preceding studies on oxalato-bridged Cr^{III}–M^{II} compounds (M = Cu, Ni, Co, Fe, Mn) in which the oxalato adopts a bisbidentate coordination mode and the two metal atoms are six-coordinated, reveal the occurrence of weak intramolecular ferromagnetic coupling.[5,23,55] This ferromagnetic coupling through bisbidentate oxalate can be

explained on simple orbital symmetry considerations. The chromium(III) ion in O_h symmetry has three unpaired electrons on the t_{2g} orbitals whereas the Cu^{II} and Ni^{II} have unpaired electrons only on the e_g orbitals (e_g^1 and e_g^2 for Cu^{II} and Ni^{II}, respectively). Consequently, the overlap for the t_{2g}^3–e_g^1 Cr^{III}–ox–Cu^{II} and t_{2g}^3–e_g^2 Cr^{III}–ox–Ni^{II} cases is zero (classical examples of strict orthogonality between the magnetic orbitals involved in the bimetallic unit) and ferromagnetic coupling arises, as observed. For the three other cases [t_{2g}^3–$t_{2g}^5e_g^2$ (Cr^{III}–ox–Co^{II}), t_{2g}^3–$t_{2g}^4e_g^2$ (Cr^{III}–ox–Fe^{II}) and t_{2g}^3–$t_{2g}^3e_g^2$ (Cr^{III}–ox–Mn^{II})], net overlapping between the t_{2g}–t_{2g} orbitals (and thus an antiferromagnetic contribution) is also involved, in addition to the above specified ferromagnetic one. As both contributions have opposite signs, the overall coupling will depend on their relative magnitudes. In light of the reported results through bisbidentate oxalato, the ferromagnetic contribution is somewhat stronger and a weak ferromagnetic coupling is observed for this family of bimetallic complexes. In the case of **3**, the lower symmetry of the oxalato bridge (bidentate towards Cr^{III} and monodentate towards Mn^{II}) should decrease the efficiency of the ferromagnetic pathway and the antiferromagnetic one becomes dominant.

In summary, the building block of formula $[Cr(phen)(ox)_2]^-$ has been prepared and structurally characterized (complex **1**) and its complexing ability towards sodium(I) (complex **2**) and manganese(II) (complex **3**) metal ions tested. The sheetlike polymer **2** and the tetranuclear complex **3** with two bridging modes of oxalate (bisbidentate oxalate and bisbidentate/monodentate) (**2**) and three coordination modes of oxalate (terminal bidentate and bridging bisbidentate and bidentate/monodentate) (**3**) are obtained. Antiferromagnetic coupling between Cr^{III} and Mn^{II} through the unprecedented chelating/monodentate bridging oxalato is reported.

Acknowledgements

Financial support from the Spanish Dirección General de Investigación Científica y Técnica (DGICYT) through Project PB97-1397, the Romanian Ministry of Education (Grants 30C/CNCSIS and 1D/CMCSIS), the TMR Program from the European Union (Contract ERBFMRXCT98-0181) and the COST Program (Action 518) is gratefully acknowledged. Thanks are also extended to the Centre d'Informàtica de la Universitat de València for computer resource support.

References

1 O. Kahn, *Adv. Inorg. Chem.*, 1995, **43**, 179.
2 S. Decurtins, R. Pellaux, A. Hauser and M. E. von Arx, in *Magnetism: A Supramolecular Function*, ed. O. Kahn, NATO ASI Series C484, Kluwer, Dordrecht, 1996, pp. 487–508.
3 S. Decurtins, H. W. Schmalle, R. Pellaux, P. Fischer and A. Hauser, *Mol. Cryst. Liq. Cryst.*, 1997, **305**, 227 and references therein.
4 S. Decurtins, S. Ferlay, R. Pellaux, M. Gross and H. Schmalle, in *Supramolecular Engineering of Synthetic Magnetic Materials*, eds. J. Veciana, C. Rovira and D. B. Amabilino, NATO ASI Series C518, Kluwer, Dordrecht, 1999, pp. 175–196.
5 Y. Pei, Y. Journaux and O. Kahn, *Inorg. Chem.*, 1989, **28**, 100.
6 H. Tamaki, Z. J. Zhong, N. Matsumoto, S. Kida, M. Koikawa, N. Achiwa, Y. Hashimoto and H. Okawa, *J. Am. Chem. Soc.*, 1992, **114**, 6974.
7 L. O. Atovmyan, G. V. Shilov, R. N. Lyubovskaya, E. I. Zhilaeva, N. S. Ovanesyan, S. I. Pirumova and I. G. Gusakovskaya, *JETP Lett. Engl. Transl.*, 1993, **58**, 766.
8 S. Decurtins, H. W. Schmalle, H. R. Oswald, A. Linden, J. Ensling, P. Gütlich and A. Hauser, *Inorg. Chim. Acta*, 1994, **216**, 65.
9 S. Decurtins, H. W. Schmalle, P. Schneuwly, J. Ensling and P. Gütlich, *J. Am. Chem. Soc.*, 1994, **116**, 9521.
10 W. M. Reiff, J. Kreisz, L. Meda and R. U. Kirss, *Mol. Cryst. Liq. Cryst.*, 1995, **273**, 181.
11 R. P. Farrell, T. W. Hambley and P. A. Lay, *Inorg. Chem.*, 1995, **34**, 757.
12 P. Román, C. Guzmán–Miralles and A. Luque, *J. Chem. Soc., Dalton Trans.*, 1996, 3985.
13 C. Mathonière, C. J. Nuttall, S. G. Carling and P. Day, *Inorg. Chem.*, 1996, **35**, 1201.
14 S. G. Carling, C. Mathonière, P. Day, K. M. Abdul Malik, S. J. Coles and M. B. Hursthouse, *J. Chem. Soc., Dalton Trans.*, 1996, 1839.
15 S. Decurtins, H. W. Schmalle, R. Pellaux, P. Schneuwly and A. Hauser, *Inorg. Chem.*, 1996, **35**, 1451.
16 M. Clemente–León, E. Coronado, J. R. Galán–Mascarós and C. Gómez–García, *Chem. Commun.*, 1997, 1727.
17 S. Decurtins, M. Gross, H. W. Schmalle and S. Ferlay, *Inorg. Chem.*, 1998, **37**, 2443.
18 M. Hernández–Molina, F. Lloret, C. Ruiz–Pérez and M. Julve, *Inorg. Chem.*, 1998, **37**, 4131.
19 T. Sanada, S. Suzuki, T. Yoshida and S. Kaizaki, *Inorg. Chem.*, 1998, **37**, 4712.
20 R. Pellaux, H. W. Schmalle, R. Huber, P. Fischer, T. Hauss, B. Ouladdiaf and S. Decurtins, *Inorg. Chem.*, 1997, **36**, 2301.
21 S. Decurtins, H. W. Schmalle, R. Pellaux, R. Huber, P. Fischer and B. Ouladdiaf, *Adv. Mater.*, 1996, **8**, 647.
22 F. Lloret, M. Julve, M. Mollar, I. Castro, J. Latorre and J. Faus, *J. Chem. Soc., Dalton Trans.*, 1989, 729.
23 M. Ohba, H. Tamaki, N. Matsumoto and H. Okawa, *Inorg. Chem.*, 1993, **32**, 5385.
24 M. C. Muñoz, M. Julve, F. Lloret, J. Faus and M. Andruh, *J. Chem. Soc., Dalton Trans.*, 1998, 3125.
25 M. Andruh, R. Melanson, C. V. Stager and F. D. Rochon, *Inorg. Chim. Acta*, 1996, **251**, 309.
26 F. D. Rochon, R. Melanson and M. Andruh, *Inorg. Chem.*, 1996, **35**, 6086.
27 N. Stanica, C. V. Stager, M. Cimpoesu and M. Andruh, *Polyhedron*, 1998, **17**, 1787.
28 G. De Munno, D. Armentano, M. Julve, F. Lloret, R. Lescouëzec and J. Faus, *Inorg. Chem.*, 1999, **38**, 2234.
29 F. Bérézovsky, A. A. Hajem, S. Triki, J. Sala Pala and P. Molinié, *Inorg. Chim. Acta*, 1999, **284**, 8.
30 K. Nakamoto, *Infrared and Raman Spectra of Inorganic and Coordination Compound*, Wiley, New York, 4th edn., 1986, p. 228.
31 A. Earshaw, *Introduction to Magnetochemistry*, Academic Press, London, 1968.
32 (*a*) G. M. Sheldrick, *SHELX 86, A Program for Crystal Structure Determination*, University of Göttingen, Göttingen, Germany, 1986; (*b*) G. M. Sheldrick, *SHELX 93, A Program for the Refinement of Crystal Structures*, University of Göttingen, Göttingen, Germany, 1993.
33 *International Tables for X-ray Crystallography*, Kynoch Press, Birmingham, 1974, vol. 4, p. 99.
34 C. K. Jonhson, *ORTEP*, Report ORNL-3794, Oak Ridge National Laboratory, Oak Ridge, TN, 1971.
35 N. Sakagami, E. Kita, P. Kita, J. Wísniewska and S. Kaizaki, *Polyhedron*, 1999, **18**, 2001.
36 R. P. Scaringe, P. Singh, R. P. Eckberg, W. E. Hatfield and D. J. Hodgson, *Inorg Chem.*, 1975, **14**, 1127.
37 J. T. Veal, W. E. Hatfield and D. J. Hodgson, *Acta Crystallogr., Sect. B*, 1973, **29**, 12.
38 S. Nishigaki, H. Yoshioka and K. Nakatsu, *Acta Crystallogr., Sect. B*, 1978, **34**, 875.
39 (*a*) J. Baldas, S. F. Colmanet and M. F. MacKay, *J. Chem. Soc., Dalton Trans.*, 1988, 1725; (*b*) R. Vicente, J. Ribas, S. Alvarez, A. Seguí, X. Solans and M. Verdaguer, *Inorg. Chem.*, 1987, **26**, 4004; (*c*) R. Grenz, F. Götzfried, U. Nagel and W. Beck, *Chem. Ber.*, 1986, **119**, 1217.
40 I. Dance and M. Scudder, *Chem. Eur. J.*, 1996, **2**, 481.
41 I. Dance and M. Scudder, *J. Chem. Soc., Dalton Trans.*, 1998, 1341.
42 (*a*) J. Cano, G. DeMunno, J. Sanz, R. Ruiz, F. Lloret, J. Faus and M. Julve, *J. Chem. Soc., Dalton Trans.*, 1994, 3465; (*b*) D. Deguenon, G. Bernardelli, J. P. Tuchagues and P. Castan, *Inorg. Chem.*, 1990, **29**, 3031; (*c*) S. Ménage, S. E. Vitols, P. Bergerat, E. Codjovi, O. Kahn, J. J. Girerd, M. Guillot, X. Xolans and T. Calvet, *Inorg. Chem.*, 1991, **30**, 2666; (*d*) J. H. Jiang, S. L. Ma, D. Z. Liao, S. P. Yan, G. L. Wang, X. K. Yao and R. J. Wang, *J. Chem. Soc., Chem. Commun.*, 1993, 745; (*e*) M. Andruh, H. W. Roesky, M. Noltemeyer and H. G. Schmidt, *Polyhedron*, 1993, **12**, 2901; (*f*) H. Oshio, E. Ino, I. Mogi and T. Ito, *Inorg. Chem.*, 1993, **32**, 5697.

43 R. Deyrieux, C. Berro and A. Péneloux, *Bull. Soc. Chim. Fr*., 1973, **1**, 25.
44 K. Wieghardt, U. Bossek, B. Nuber, J. Weiss, J. Bonvoisin, M. Corbella, S. E. Vitols and J. J. Girerd, *J. Am. Chem. Soc*., 1998, **110**, 7398.
45 L. L. Merrit and E. D. Schroeder, *Acta Crystallogr*., 1956, **9**, 801.
46 C. J. O'Connors, *Prog. Inorg. Chem*., 1986, **29**, 203.
47 A. J. Amoroso, J. C. Jeffery, P. L. Jones, J. A. McCleverty, P. Thornton and M. D. Ward, *Angew. Chem., Int. Ed. Engl*., 1995, **34**, 1443.
48 M. E. Lines, *J. Phys. Chem. Solids*, 1970, **31**, 101.
49 M. Verdaguer, *Ph. D. Thesis*, University of Orsay, France, 1984.
50 J. Glerup, P. A. Goodson, D. J. Hodgson and K. Michelsen, *Inorg. Chem*., 1995, **34**, 6255.
51 (*a*) T. R. Felthouse, E. J. Laskowski and D. N. Hendrickson, *Inorg. Chem*., 1977, **16**, 1077; (*b*) M. Julve, M. Verdaguer, A. Gleizes, M. Philoche–Levisalles and O. Kahn, *Inorg. Chem*., 1984, **23**, 3808; (*c*) P. Román, C. Guzmán–Miralles, A. Luque, J. I. Beitia, J. Cano, F. Lloret, M. Julve and S. Alvarez, *Inorg. Chem*., 1996, **35**, 3741 and references therein.
52 M. F. Charlot, M. Verdaguer, Y. Journaux, P. de Loth and J. P. Daidey, *Inorg. Chem*., 1984, **23**, 3802.
53 S. Alvarez, M. Julve and M. Verdaguer, *Inorg. Chem*., 1990, **29**, 4500.
54 J. Cano, P. Alemany, S. Alvarez, M. Verdaguer and E. Ruiz, *Chem. Eur. J*., 1998, **4**, 476.
55 M. Ohba, H. Tamaki, N. Matsumoto, H. Okawa and S. Kida, *Chem. Lett*., 1991, 1157.